Deposition and Wettability of [bmim][triflate] on Self-Assembled Monolayers

Angeline M. Cione, Oleg A. Mazyar, Brandon D. Booth, Clare McCabe,* and G. Kane Jennings*

Department of Chemical and Biomolecular Engineering, Vanderbilt University, Nashville, Tennessee 37235

Received: September 11, 2008; Revised Manuscript Received: December 8, 2008

The interfacial behavior of ionic liquids (ILs) affects their use in many applications including as solvents, electrolytes, and lubricants. Here, we report the wettability and deposition of 1-*n*-butyl-3-methylimidazolium triflate ([bmim][triflate]) on model surfaces generated by the assembly of thiol- and silane-based monolayers on gold and silicon, respectively. Advancing contact angles of [bmim][triflate] on $-CF_3$, $-CH_3$, $=CH_2$, $-OH$, and mixed $-CH_3/-OH$ surfaces are found to be intermediate between those of water and hexadecane on the same surfaces and dissimilar to those of dicyclohexyl, which has a similar surface tension as [bmim][triflate] but only dispersive intermolecular interactions. Molecular simulations provide qualitative agreement with experimental contact angles and show that the hydroxyl surface disrupts electrostatic interactions between the ions of the [bmim][triflate] droplet, resulting in lower local surface tensions and increased area of contact. IL films as thin as ~100 nm were prepared by casting [bmim][triflate] from ethanol at reduced pressures onto mixed $-CH_3/-OH$ surfaces. Coherent films of [bmim][triflate] were achieved only beyond a critical surface energy corresponding to advancing [bmim][triflate] contact angles of $\leq 25°$ and advancing water contact angles of $\leq 70°$. Comparison of infrared vibrational spectra of the IL as a thin film, versus those for thicker films and in the bulk, suggests an interfacially driven structuring of the ions in the thinnest films and is supported by simulations, which show that the CF_3 groups of the triflates orient away from the IL phase at the IL/vacuum interface.

Introduction

Room temperature ionic liquids (ILs) typically contain a bulky, asymmetric organic cation that inhibits crystalline packing and results in low melting temperatures.[1] ILs can exhibit other significant properties including negligibly low vapor pressure, noncombustibility, and a broad range of electrochemical stability.[2] ILs are truly uniquely flexible chemicals in that their properties can be tuned by varying the cation or anion. Thus, by altering the structure of the ions or choosing different cation−anion combinations, an ionic liquid with desirable properties for a specific application could be designed or selected. Because of their useful properties and tunability, ILs have found many applications including use as nonvolatile solvents,[3] electrolytes,[4] chromatographic stationary phases,[5] and lubricants.[6−8] In addition to lubrication, the versatility and unique properties of ILs make them good candidates for many applications that involve interactions of liquids with surfaces. For these applications to be realized, efficient methods of depositing thin films of ILs must be developed.

In this paper, we investigate the deposition and spreading of 1-*n*-butyl-3-methylimidazolium triflate ([bmim][triflate]) (Figure 1) on model surfaces generated by the assembly of thiol- and silane-based monolayers on gold and silicon, respectively. Imidazolium-based ILs are the most commonly studied IL system to date because of their air and moisture stability.[2,9] While the bulk-phase viscosity of ILs can be comparable to traditional hydrocarbon lubricants, ILs have been shown to exhibit superior antiwear and friction-reducing properties in lubrication settings.[10−12] In particular, ILs with the 1-*n*-alkyl-3-methylimidazolium cation and either the BF_4 or PF_6 anion have proven to be effective lubricants in many studies;[7,8,13−15] however, these anions hydrolyze upon exposure to water. More recently, Jimenez et al.[15] have shown that the triflate anion, CF_3SO_3, has better wear-reducing properties than BF_4 or PF_6 and that cations with longer side chains ($n > 2$) improved wear properties more than changing the anion. The selection of [bmim][triflate] in the present study is further driven by its ease of preparation[3] as well as its relatively low viscosity (90 cP at 20 °C)[5] and surface tension (34 mN/m at 22 °C) when compared against some other ILs in the imidazolium family.[5]

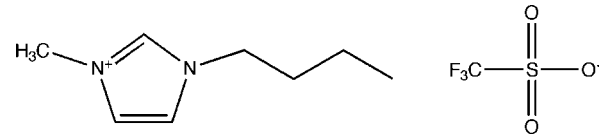

Figure 1. Chemical structure of [bmim][triflate].

For a liquid to effectively form a thin film, it must be compatible with the underlying surface,[16] meaning the liquid must readily spread across the surface. Spreading behavior of a liquid is described by[17]

$$S = \gamma_{SV} - (\gamma_{SL} + \gamma_{LV}) \geq 0 \quad (1)$$

where S is the spreading coefficient, γ_{SV} describes the surface energy of the solid, γ_{LV} is the surface tension of the liquid, and γ_{SL} is the interfacial free energy at the solid−liquid interface. Thus, increasing surface energy, γ_{SV}, and decreasing surface tension, γ_{LV}, both promote spreading or film formation. The surface tension is a property inherent to the liquid; the surface energy is a property inherent to the solid surface and can be varied by modifying the surface to contain appropriate

* Authors to whom correspondence should be addressed. E-mail: kane.g.jennings@vanderbilt.edu and c.mccabe@vanderbilt.edu. Phone: (615)322-2707(G.K.J.) and (615)322-6853(C.M.). Fax: (615)343-7951 (G.K.J. and C.M.).

10.1021/jp808098w CCC: $40.75
Published on Web 01/20/2009

functional groups.[18] Here, we use self-assembled monolayers (SAMs) of ω-terminated alkyl thiols on gold as well as monolayers prepared by alkyl trichlorosilanes on silicon oxide as molecularly thin films to modify surface properties from low energy (hydrophobic) to high energy (hydrophilic) and enable the investigation of wettability and spreading by ionic liquids into thin films.

Gao and McCarthy[19] have reported the wettability of four different ILs with surface tensions ranging from 49 to 66 mN/m on various hydrophobic and superhydrophobic surfaces. They noted the complexity of contact angle analysis with ILs since either ion of the probe liquid can interact with the surface. For the ultralow energy surfaces, the contact angles of the ILs were often indistinguishable from those of water. For a typical smooth polymer, the contact angles of the ILs were lower than that of water, owing to their lower surface tensions. In this work, we use contact angle goniometry to measure the wettability of [bmim][triflate] on several model 2-D surfaces, ranging from low energy to high energy, prepared by the assembly of normal and ω-terminated alkyl thiols on gold and alkyl trichlorosilanes on silicon (oxide). We combine these experiments with molecular simulations to investigate the composition and structuring of the ions within a droplet and near the interfaces. This information on IL wettability is then correlated with the spreading of [bmim][triflate] on mixed monolayers that span a range of wettability. Optical microscopy is used to assess the spreading of the IL into a film, and reflectance−absorption infrared spectroscopy (RAIRS) is used to investigate the composition and structuring within the IL films.

Experimental Methods

Materials. All water was deionized (DI), purified to 16.7 MΩ·cm with a Modu-Pure system. Compressed N_2 was obtained from J&M Cylinder Gas, Inc. Anhydrous dichloromethane and anhydrous toluene were purchased from Fisher. Anhydrous chloroform (99%), methyl trifluoromethane sulfonate (98%), butyl imidazole (98%), anhydrous THF, borane−THF complex, ammonium hydroxide, dicyclohexyl (99%), hexadecane (99%), 1-octadecanethiol, 1-dodecanethiol, 1-octanethiol, and 11-mercapto-1-undecanol were purchased from Sigma-Aldrich and used as received. (Tridecafluoro-1,1,2,2-tetrahydrooctyl)-1-trichlorosilane, octyltrichlorosilane, and octadecyltrichlorosilane were purchased from United Chemical Technologies (UCT) and used as received. 5-Hexenyltrichlorosilane, 7-octenyltrichlorosilane, dodecyltrichlorosilane, and hexadecyltrichlorosilane were purchased from Gelest and used as received. Silicon wafers (100) were purchased from Montco Silicon. NaCl crystals and coverslips (used to do transmission IR spectroscopy on the ionic liquid) were from International Crystal Laboratories.

Procedures. ***[bmim][triflate] (IL) Preparation.*** The procedure for the synthesis of the ionic liquid, [bmim][triflate], was adapted from a procedure reported by Bonhote et al.[20] Under nitrogen atmosphere, ∼120 mL of anhydrous dichloromethane was added to 50 g of methyl triflate (0.3 mol) to prepare a ∼2.5 M solution. This methyl triflate solution was added dropwise to 42 mL (∼0.3 mol, or 38 g) of 1-butylimidazole under a nitrogen atmosphere and stirred vigorously in an ice bath. Solvent was removed by placement of the single phase liquid on a rotary evaporator followed by placement of the liquid on the vacuum line overnight. The final product was stored under nitrogen atmosphere and characterized by using ^{1}H NMR analysis, which revealed no water in the final product. ^{1}H NMR (400 MHz, $CDCl_3$) δ 0.916 (3H), 1.30 (2H), 1.83 (2H), 3.93 (3H), 4.16 (2H), 7.38 (2H), 9.03 (1H).

Surface Preparation on Silicon. Substrates were prepared from Si wafers and cut into ∼4 cm × 1.3 cm pieces. The samples were sonicated in soapy water for 30 min, rinsed with water, dried, and placed in piranha solution (14 mL of H_2SO_4:6 mL of H_2O_2) for 30 min to 1 h to remove adventitious carbon and hydroxylate the SiO_2 into silanols that are reactive toward trichlorosilane head groups. Samples were rinsed three times by submersion in water. The first rinse was a 15 s submersion/agitation, followed immediately by submersion in a second rinse for 10 min, and a final submersion that lasted ∼10−30 min. All samples were rinsed once more with DI water and thoroughly dried with N_2 before submersion into the precursor solution.

Precursor Solutions and Monolayer Preparation. For monolayer formation on silicon surfaces, 1 mM solutions of the alkyltrichlorosilane precursor in anhydrous toluene were prepared. This solvent was chosen because solvents with few or no methylene groups are known to interfere less with the packing of the alkyl chains, allowing close-packed, well-ordered monolayers to be formed.[21] Much care was taken to keep water out of these solutions, and thus samples were thoroughly dried in a stream of N_2 before submersion because water in these systems promotes polymerization of silanes, preventing well-packed monolayers from being formed.[22] While a small amount of water on the surface appears to lead to a higher film density,[23−25] the increased density is likely due to vertical polymerization rather than a more closely packed monolayer.[22,26,27] An exposure time of ∼5 h in solution yielded the most oleophobic surface without yielding thicknesses that suggested the presence of vertical polymerization (Supporting Information).

To deposit self-assembled monolayers onto gold, evaporated gold substrates were exposed to 1 mM solutions of an alkanethiol in ethanol for at least 24 h. For mixed monolayers, precursor solutions of *n*-dodecanethiol ($C_{12}SH$) with varying proportions of mercapto-1-undecanol ($HOC_{11}SH$) were prepared such that each mixture had a total thiol concentration of 1 mM. Initially, mixtures of 0, 20%, 40%, 60%, 80%, and 100% (molar) $HOC_{11}SH$ were prepared from stock solutions of $C_{12}SH$ and $HOC_{11}SH$. To hone in on the critical composition that yielded a surface that would accept an ionic liquid film, mixtures of 80%, 85%, 90%, 95%, and 100% (molar) $HOC_{11}SH$ were later prepared from new stock solutions. Finally, mixtures of 91%, 92%, 93%, and 94% (molar) $HOC_{11}SH$ were prepared from the latter stock solution. Two gold samples were placed in each solution for 24 h. Drop casting or contact angle analysis was performed immediately upon removing samples from solution and rinsing with water and drying in a stream of nitrogen.

To vary the surface energy of silane monolayers, a hydroboration−oxidation (HB-O) reaction was performed.[28] Piranha-treated silicon samples were submerged in a 1 mM solution of varying ratios of *n*-octyltrichlorosilane and 7-octenyltrichlorosilane in anhydrous toluene for 1−3 h. Immediately upon removal from solution, samples were characterized or oxidized in the following manner. Under nitrogen atmosphere, the samples were treated with 1.0 M borane·THF complex solution for 10−20 min and rinsed with anhydrous THF. Samples were then removed from the nitrogen atmosphere, rinsed with copious amounts of water, and submerged in a heated (1:1:5) solution of ammonium hydroxide, H_2O_2, and water for up to 1 h. Immediately upon removal from the hydroxide solution, samples were rinsed with copious amounts of water, dried, and either characterized or coated by drop casting.

TABLE 1: Measured Surface Tensions by the Wilhelmy Plate Method for the Liquids Used in This Study

liquid	surface tension (mN/m)	temp (°C)
ethanol	23	19
hexadecane	27	20
dicyclohexyl[a]	33	22
[bmim][triflate]	34	22
water	72	21

[a] From ref 47.

The advancing water contact angle of each sample was measured to estimate the fractional surface coverage of the monolayer from the equation proposed by Cassie,[29]

$$\cos\theta_{\text{mixed}} = \sigma_1 \cos(\theta_1) + (1-\sigma_1)\cos(\theta_2) \qquad (2)$$

where θ_{mixed} is the water contact angle on the mixed monolayer, σ_i is the fractional coverage of species i in the monolayer, and θ_i is the water contact angle on a surface with 100% species i.

Drop Casting. A solution of 0.5% (w/v) IL in ethanol was prepared for drop casting. A plastic weigh boat was placed upside down in a 25 mL Erlenmeyer flask to provide a flat platform for the samples. Samples were placed on the platform, and a 10 μL drop was deposited in the center of the sample. The flask was immediately capped with a septum, secured with wire, and a needle was inserted into the septum to pull a vacuum on the flask. The flask was left under vacuum until the solvent was fully evaporated. To examine the effects of drop casting from varying IL solution concentrations, the area of spreading was confined to 1 cm^2 by clamping the substrate into a Flat Cell (EG&G Instruments). The sample was secured in the stage, a drop of IL solution was applied to the exposed sample area, and a septum was held over the exposed area. The needle was inserted into the septum and a vacuum was pulled in the confined volume over the sample surface.

Characterization Techniques. ***Suface Tension of [bmim][triflate].*** Surface tension measurements were performed on a KSV Sigma 701 Tensiometer, which was controlled by KSV Instruments 70 software (Table 1). A platinum Wilhelmy plate was suspended from an electrobalance with a measuring resolution of 1 μN. The Wilhelmy plate was lowered to touch the surface of the liquid and then submerged a specified distance into the liquid. The balance was zeroed and then the force required to remove the plate from the liquid at a constant speed was recorded. The platinum Wilhelmy plate was 0.1 mm thick and 19.6 mm long, giving a wetted length of 39.4 mm. The plate was raised and lowered at a rate of 20.0 mm/min and submerged to a depth of 5.0 mm in the liquid. Before testing of the ionic liquid, absolute ethanol, hexadecane, and water were tested to ensure the accuracy of the instrument. Approximately 10 mL of liquid was needed to perform the experiment and values represent 5 separate runs with each run consisting of at least 10 measurements taken at 1 min intervals.

Wettability. Advancing and receding contact angles were measured on static ~5 μL drops with a Rame-Hart goniometer, using a syringe to apply DI water, hexadecane, dicyclohexyl, or [bmim][triflate] (IL) as the probe fluid. The needle of the syringe remained inside the probe fluid droplet as the advancing and receding contact angle measurements were taken.

Film Thicknesses. Film thicknesses were measured with a J.A. Woollam XLS-100 variable angle spectroscopic ellipsometer. For each sample, 200 revs/meas were taken across a wavelength range of 400−600 nm at a 75° angle of incidence. WVASE 32 Version 3.374 software was used to model and calculate the thickness of the oxide layer and films. For monolayers grown from a silicon surface, the surface was modeled as a 0.5 mm Si substrate with an oxide layer (modeled using the software's "SiO_2" file) and a Cauchy layer. The thickness of the oxide layer was approximated with a "point-by-point" fit on a piranha-treated Si substrate. The thicknesses of the monolayers were determined by fits of the data by the model, using a "point-by-point" fit approximating the index of refraction as 1.46. (The second Cauchy coefficient, B, was set to zero.) For substrates that had an IL film applied to them, the thickness of the first film was calculated and saved before a second, decoupled Cauchy layer was applied to the model and data were fitted by using the same procedure. For monolayers on gold, a fresh, uncoated sample of gold was scanned, and a Cauchy fit of the n and k values was used to model the substrate. The monolayer thickness was approximated by using the Cauchy model with the coefficients set at $A = 1.46$ and $B = C = 0$. The thickness of the IL coatings on gold was approximated by using the Cauchy model with coefficients set to $A = 1.434$ and $B = C = 0$.

Reflectance−Absorption Infrared Spectroscopy (RAIRS). RAIRS was performed with a Varian Excalibur FTS-3000 infrared spectrometer with p-polarized light incident at 80° from the surface normal. Reflected light was detected with a nitrogen-cooled, narrow-band MCT detector. A background spectrum was accumulated on a gold substrate that was pre-exposed to deuterated n-dodecanethiol ($C_{12}D_{25}SH$). A second spectrum of this same sample was accumulated after it had been exposed to ambient air for a few seconds, and this new spectrum was subtracted from the spectrum of all films to eliminate peaks due to ambient humidity. A spectrum of the bulk IL was acquired in transmission mode. A background spectrum was obtained with a clean NaCl crystal. A water spectrum was obtained by exposing the NaCl crystal to the ambient humidity for a few seconds before obtaining another spectrum. A drop of IL was then placed on a NaCl crystal, and a transmission spectrum was immediately obtained by using about 10 scans. The water spectrum was subtracted from the spectrum of the IL film to account for ambient humidity.

Optical Microscopy. Microscope images of the IL thin films were acquired with an Olympus BX41 microscope with Pixera camera and Pixera Viewfinder Pro software.

Molecular Simulation. The simulation setup for a [bmim][triflate] drop on the surface of an alkylsilane monolayer chemically bonded to the SiO_2 surface is shown in Figure 2. Two types of monolayers chemically bonded through the Si atom in the $Si(OH)_2$ group to the O atom of the SiO_2 surface were considered: chains with 8 CH_2 groups and a terminal CH_3 group (see Figure 2a) and chains in which the terminal methyl groups are substituted by hydroxyl groups (Figure 2b). The SiO_2 surface is represented by a structure obtained from thermal equilibration of an ideal β-cristobalite[30,31] with a lattice constant of 5.07 Å at 300 K and is composed of 6 Si atoms and 6 O atom layers arranged in a hexagonal lattice of SiO_4 tetrahedra alternatively pointing up and down. The model surface is 87.8 Å × 86.1 Å and is obtained by cutting the β-cristobalite crystal above the layer of O atoms at the top of the upward SiO_4 tetrahedra.[32] Each O atom of this layer is bonded to one Si atom of the alkylsilane chain forming a full coverage monolayer that contains 340 $Si(OH)_2(CH_2)_8CH_3$ or $Si(OH)_2(CH_2)_8OH$ chains and satisfies both bonding and steric constraints.[32,33] In this model, the area per chain is ~22.2 Å^2, which is in good agreement with experimental values of 22−25 Å^2 for monolayers formed on amorphous silica at full coverage.[34−36] We note, however, that the crystalline substrate used in the

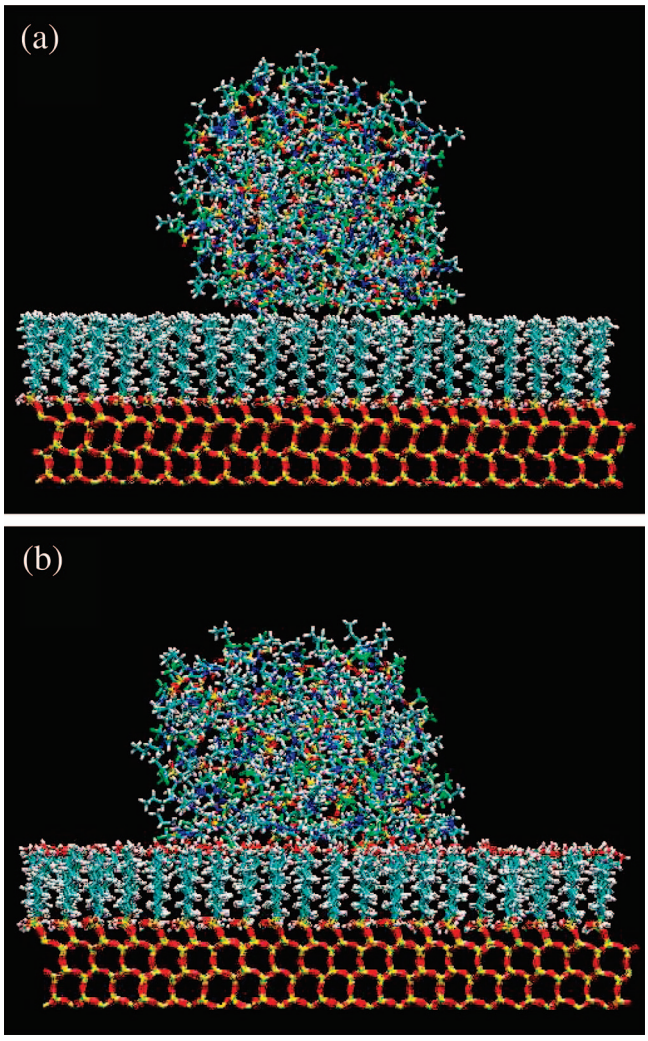

Figure 2. Snapshots from molecular simulations of a [bmim][triflate] droplet taken at $t \approx 0.5$ ns on (a) a hydrophobic $Si(OH)_2(CH_2)_8CH_3$ and (b) a hydrophilic $Si(OH)_2(CH_2)_8OH$ monolayer on silica.

simulations allows for ~10% tighter chain packing than the experimental amorphous SiO_2 surfaces.[32]

A near-spherical IL drop consisting of 100 [bmim][triflate] molecules with an average radius of ~19 Å was prepared from a 1 ns equilibration at 300 K of ions randomly placed in a 30 × 30 × 30 Å^3 box. The drop was then placed above the monolayer-covered SiO_2 surface with a 1.25 Å gap between the drop and the surface. The whole system was then further equilibrated for 200 ps.

The OPLS all-atom force field[37] and its extension for crystalline silicon oxide[38] was used to describe the interactions within the monolayer-coated β-cristobalite surface. The transferable molecular force fields of Cadena et al.[39] and Canongia Lopes et al.[40] were used to model the [bmim] cations and [triflate] anions, respectively. The long-range interactions between the cations, anions, and the surface were computed by using a damped shifted force method,[41] which is a development of the damped and cutoff-neutralized Coulombic sum originally proposed by Wolf et al.[42] For the electrostatic calculations, a damping parameter of 0.2 Å^{-1} and a cutoff radius of 15 Å were used.[41] A large cutoff distance of 13.5 Å was employed for accurate computation of the Lennard-Jones interactions.

Molecular dynamics (MD) simulations were performed by using the multiple time step rRESPA[43] algorithm with a 0.25 fs time step for bond, valence, dihedral, and improper angle forces and 1.0 fs for the intra- and intermolecular nonbonding forces. The lowest layer of Si atoms in the surface was held rigid and 2D periodic boundary conditions were applied during the simulations. During a 200 ps initial equilibration period, the whole system (excluding the rigid Si atom layer of the surface) was coupled to a 300 K Berendsen thermal bath.[44] Subsequently during production runs, only the four bottom atomic layers of the SiO_2 surface adjacent to the rigid layer were connected to the thermostat.

TABLE 2: Contact Angles (Advancing, Receding) for SAMs on Au and Si

adsorbate/substrate	θ_{H_2O}[a] (deg)	θ_{HD}[b] (deg)	θ_{DCH}[a] (deg)	θ_{IL}[a] (deg)
$C_{18}SH/Au$	112, 102	49, 40	56, 45	69, 64
$C_{12}SH/Au$	109, 96	46, 30	54, 44	64, 60
C_8SH/Au	106, 98	43, 32	47, 38	66, 58
$HOC_{11}SH/Au$	28, 19	<15	20	17
$C_{18}SiCl_3/SiO_2$	109, 103	44, 40	49, 44	69,65
$C_{12}SiCl_3/SiO_2$	111, 103	37, 32	45, 40	72, 64
C_8SiCl_3/SiO_2	109, 100	32, 26	38, 31	67, 56
$F_3C(CF_2)_5(CH_2)_2SiCl_3/SiO_2$	125, 75[c]	80, 55[d]	81, 57	91, 57
$H_2C{=}C_5H_9SiCl_3/SiO_2$	96, 84[c]	<15[d]	<15	50, 33
(HB-O) $H_2C{=}C_5H_9SiCl_3/SiO_2$	57, 32	<15[d]	<15	19

[a] Standard deviation ±4. [b] Standard deviation ±1. [c] Standard deviation ±10. [d] Standard deviation ±5.

Results and Discussion

Wettability of Monolayers on Gold and Silicon. Monolayers of varying thickness and surface functionality were assembled onto gold from *n*-alkanethiols ($CH_3(CH_2)_{n-1}SH$; n = 8, 12, and 18) and 11-mercapto-1-undecanol ($HOC_{11}SH$). Monolayers of varying thickness and surface functionality were formed on piranha-treated silicon wafers, using *n*-alkyltrichlorosilanes ($CH_3(CH_2)_{n-1}SiCl_3$; n = 8, 12, and 18), (tridecafluoro-1,1,2,2-tetrahydrooctyl)-1-trichlorosilane ($F_3C(CF_2)_5(CH_2)_2SiCl_3$), and 5-hexenyltrichlorosilane ($H_2C{=}C_5H_{10}SiCl_3$), before and after hydroboration/oxidation, in anhydrous toluene. To ensure that monolayer films were produced from the silanes, which have a tendency to polymerize vertically under nonoptimal conditions,[45] the ellipsometric thicknesses of films prepared from *n*-alkyltrichlorosilanes were measured and observed to exhibit appropriate monolayer thicknesses and to increase by ~1.3 Å with each methylene group in the alkyl chain (see Figure S1 in the Supporting Information).

To investigate the wetting properties of each monolayer formed on gold or silicon, the advancing and receding contact angles of water, hexadecane, dicyclohexyl, and [bmim][triflate] (IL) were measured and are reported in Table 2. We selected water, hexadecane (HD), and dicylcohexyl (DCH) as probe liquids due to their widespread use in other studies[46] and to compare with values obtained from [bmim][triflate]. HD (γ = 27 mN/m) and DCH (γ = 33 mN/m)[46,47] are both dispersive liquids although the surface tension of DCH is comparable to that of [bmim][triflate] (γ = 34 mN/m), which additionally has electrostatic and dipole interactions. Water has strong hydrogen bonding and a significantly higher surface tension (γ = 72 mN/m) than the other liquids studied.

The large variation in contact angles (~100° for H_2O) reflects the composition of the chain termini and indicates that these adsorbates assemble to form oriented monolayers that effectively alter the surface properties of the substrate. The highest surface energy, as evident by the lowest water contact angle, was achieved by using a hydroxyl-terminated precursor, while the lowest surface energy was achieved by using a CF_3-terminated

precursor. Methyl-terminated surfaces also yielded hydrophobic, oleophobic surfaces with low surface energies. A homogeneous methyl surface typically yields water contact angles of 109−114° [27] and hexadecane contact angles of ∼45−50°;[48] thus, the advancing water and hexadecane contact angles on monolayers formed from *n*-alkanethiols are indicative of a homogeneous methyl surface. The hexadecane contact angles on *n*-alkylsilane monolayers are lower than those on *n*-alkanethiolate monolayers suggesting that the *n*-alkanethiolate monolayers formed on Au exhibit a more homogeneous methyl surface than the monolayers formed from *n*-alkyltrichlorosilanes on silicon. Contact angles with DCH support this assertion as the methyl-terminated monolayers on gold exhibit advancing DCH contact angles that are 7−9° greater than those for methyl-terminated monolayers on silicon. The surface exposed to a precursor solution of $H_2C{=}C_5H_9SiCl_3$ exhibits wetting properties expected from a vinyl-terminated monolayer; it is hydrophobic ($\theta_{H_2O} >$ 90°), though its water contact angle is lower than that of a methyl-terminated monolayer, and it is wet by HD and DCH because the surface is composed of methylene groups that are abundant in these liquids. After undergoing a hydroboration−oxidation (HB-O) reaction, we estimate from the Cassie equation (eq 2) that two-thirds of the vinyl termini are converted to hydroxyl termini, resulting in a much lower water contact angle.

Since the surface tension of [bmim][triflate] (34 mN/m) is similar to that of DCH (33 mN/m), one might naively expect the contact angles of the IL to be similar to those of DCH. However, [bmim][triflate] contact angles are ∼10° higher than those of DCH on methyl-terminated alkanethiolate SAMs and 20−30° higher than those of DCH on methyl-terminated silane monolayers. Further, the IL shows no trend with chain length for either methyl-terminated system, unlike DCH and HD. As the HD and DCH contact angles fall significantly for thinner *n*-alkylsilane SAMs, the IL contact angle remains high. The decrease in HD and DCH contact angles for these surfaces is attributed to a greater extent of structural defects within the methyl-terminated monolayer that expose oleophilic methylene groups as the chain length is reduced. This absence of a trend in the IL contact angle suggests that the IL is less sensitive to these defects and is consistent with its presumed weak interaction with both methyl and methylene groups (vide infra). Whereas the hexadecane contact angle changes from ∼55° on a dense methyl surface to <15° on a vinyl (CH_2)-terminated surface, indicating extreme sensitivity to these functional groups, the IL contact angle decreases only from 69° to 50° for the same monolayers. The weaker sensitivity to slight changes in hydrophobic functional groups for [bmim][triflate] is more closely related to that of water and may reflect the strong electrostatic interactions between ions in the IL. Higher energy surfaces (−OH) can effectively compete for interactions with the ions of the IL, and as shown in Table 2, the values of IL and DCH contact angles are similar for these surfaces. In general, the higher energy surfaces are wet more effectively by all liquids, and thus the variation between the three probe liquids is compressed.

Simulations of IL Droplets on Surfaces. Although the contact angle can be derived from MD simulations,[49−52] as in the work of Hautman et al. and Srivastava et al.[52] for water and hexadecane on alkanethiolate SAMs on gold, we have not tried to estimate a contact angle from our simulations due to the long simulation times that would be needed given the notoriously slow dynamics of many ILs;[53] however, our simulations clearly support the experimental observation that [bmim][triflate] wets an OH-terminated surface but not a CH_3-terminated surface. As shown in Figure 2, the shape of the IL drop on the CH_3-terminated film remains close to spherical after 0.5 ns of simulation, while the shape of the drop on top of the OH-terminated film is distorted by the interactions with the surface. Furthermore, we find that the center of mass of the IL drop on the OH-terminated monolayer is 2.5 Å closer to the surface than the center of mass of the drop on the CH_3-terminated film, despite the same initial configuration, and its contact area with the surface is greater by a factor of 2 than the contact area for the drop on the CH_3-terminated surface.

Through molecular simulation we can also study the orientation of the ions and provide some insight into the nature of the molecular-level surface−IL interaction. Charge alternation, where ions of one charge are surrounded by ions of the opposite charge, is observed in the outer shells of the IL droplets, in agreement with simulations of vapor-phase IL clusters,[54] and is most likely responsible for the relatively high surface tension of the ILs. Therefore, a perturbation of this charge alternation may decrease the forces of attraction between the ions in the outer shells and, thus, reduce the surface tension in the drop. In the case of a [bmim][triflate] drop on a $Si(OH)_2(CH_2)_8OH$ monolayer (see Figure 2b), the characteristic charge alternation is perturbed by the polar hydroxyl groups on the surface. Electrostatic interactions between the OH-terminated surface and the ions of the IL drop will diminish the strength of the cation−anion interactions in the outer shell and in turn lead to a decrease in the local surface tension of the drop within the contact area of the surface, and thus to the improved wettability of the OH-terminated surface by the [bmim][triflate] IL compared to the CH_3-terminated surface. In the case of the CH_3-terminated monolayer ($Si(OH)_2(CH_2)_8CH_3$), the interactions between the IL and the surface are governed by weaker forces that do not significantly perturb the arrangement of the ions in the outer shell of the IL drop. Therefore, the surface tension in such IL drops remains strong and, as a result, the IL does not readily wet the CH_3-terminated surface.

Casting Ionic Liquid Thin Films on Monolayer Surfaces. After measuring the wettability of the IL ([bmim][triflate]) on a variety of monolayer surfaces, we investigated the effect of surface composition on the formation of IL thin films on these surfaces. To determine the critical surface energy above which a film of the IL would coat a surface, mixed self-assembled monolayers were prepared from *n*-dodecanethiol and mercaptoundecanol to create varying surface concentrations of methyl and hydroxyl termini and surfaces that range in IL contact angle from ∼70° down to ∼10°. These surfaces were subsequently coated with the IL by drop casting through a two-step process. In the first step, the IL was dissolved in ethanol at a concentration of 0.5% (w/v) and a 10 μL drop of this solution applied to the substrate. We selected ethanol due to its polarity to aid in solvating the IL and due to its low surface tension of 22 mN/m,[55] which should aid in spreading. In the second step, the substrate was immediately placed under vacuum to evaporate the ethanol. To form an IL film on the surface, the drop solution must spread across the surface, and upon evaporation, the IL should remain as a film on the surface, as depicted in Figure 3a(i). Thus, by eqs 1 and 2, the surface tension of the drop solution (IL and ethanol) must be low enough for spreading to occur, and the surface energy of the substrate must be high enough to prevent the IL from coalescing into small droplets (Figure 3a(ii)) or a large droplet (Figure 3b) upon solvent evaporation.

Figure 4 shows the IL films that were cast onto monolayers prepared from $C_{12}SH/HOC_{11}SH$ mixtures on gold. Spreading

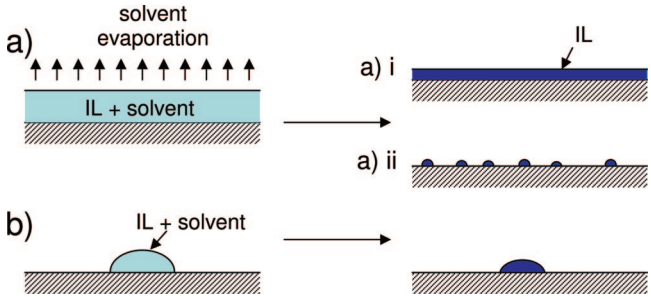

Figure 3. Behavior of the IL upon drop casting. (a) The IL/solvent drop wet the surface or (b) the IL/solvent beaded up on the surface. In IL/solvent films (a), upon evaporation (i) the IL remained as a film spread across higher energy surfaces, but on lower energy surfaces (ii) the IL coalesced into droplets scattered across the surface. In part b, the IL/solvent drop became a smaller drop of IL upon evaporation of ethanol.

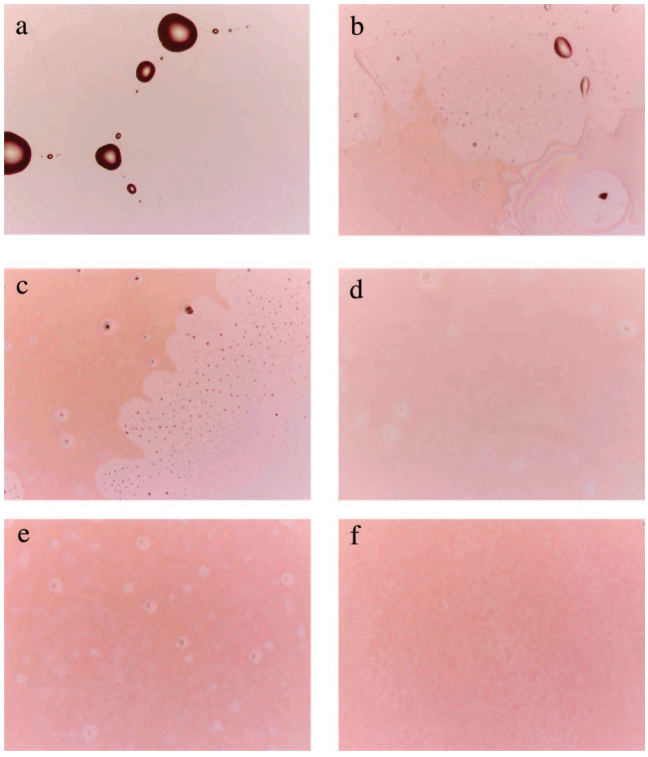

Figure 4. Optical images (5×) of IL films on mixed monolayers of methyl- and hydroxyl-terminated alkanethiols on gold: methyl surface concentration (IL contact angle) of (a) 81% (57°), (b) 54% (36°), (c) 47% (29°), (d) 43% (27°), (e) 39% (25°), and (f) 36% (20°). Data are from multiple experiments. All samples exhibited multiple regions, but the images shown here depict the most prevalent region in the specified film.

of the IL drop solution (IL + solvent) did not occur on surfaces with a fractional $C_{12}SH$ coverage of greater than 47%. However, two different wetting regimes were observed in this region. Though spontaneous spreading did not occur on surfaces with a fractional $C_{12}SH$ coverage between 47% and 87% ($29° < \theta_{IL} < 62°$), when samples were tilted, the drop moved across the surface leaving a thin film behind, suggesting that the receding contact angle of the solution (IL + solvent) on the surface was ~0°. However, due to the higher surface tension of the IL as compared to the IL drop solution (IL + solvent), after the solvent was evaporated, the IL coalesced into tiny droplets scattered across the surface, rather than spreading out into a film. In the second regime, surfaces with a fractional $C_{12}SH$ coverage of greater than 87% were never wet by the IL/ethanol drop, even

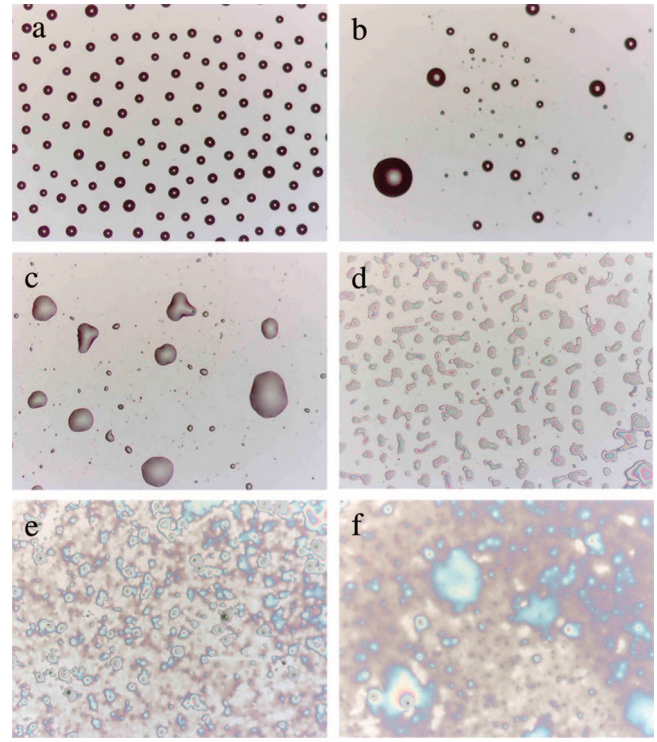

Figure 5. Optical images (5×) from IL drop cast onto modified Si surfaces with IL contact angles of (a) 57°, (b) 43°, (c) 30°, (d) 27°, (e) 24°, and (f) 20°. The films with IL contact angles <27° all contained regions of both a very continuous film and a very sparsely distributed film. The images shown here depict the most prevalent region in the specified film.

as the drop was rolled around on the surface. Under vacuum, the IL/ethanol drop shrunk into a smaller drop of IL as the ethanol evaporated. Thus, the surface energies characteristic of these two regimes are too low to be compatible with an IL film of [bmim][triflate], though the former regime is characterized by a surface energy high enough to be compatible with a film of the IL/ethanol solution. The critical fractional $C_{12}SH$ coverage in a monolayer that could be coated by an IL thin film was 45(±2)%, which corresponds to a water contact angle of ~70° and an IL contact angle of 25(±3)°. For surfaces with contact angles below this critical value, the IL spread into a film with ellipsometric thicknesses ranging from 300 to 400 nm for this 0.5% (w/v) solution when surface area was confined to 1 cm^2 and as low as ~100 nm when the area was not confined.

To determine if this critical surface condition translated to different surfaces, we prepared variations in surface energy on silicon substrates by assembling mixed vinyl/methyl-terminated silane monolayers and oxidizing the vinyl groups of the monolayer via the hydroboration−oxidation reaction. Upon drop casting and removing solvent, the IL beaded up into distinct droplets on the samples with IL contact angles greater than 30°, as shown in Figure 5. The sample with the 27° IL contact angle (Figure 5d) showed a transition state in film formation. The IL neither beaded up nor formed a continuous film. To the unaided eye, the surface appeared to have a continuous film, but microscope images showed that it consisted of tiny, closely spaced but disconnected islands of IL. Because the IL formed closely spaced islands rather than droplets, this surface must be close to the critical surface energy at which a continuous film begins to form. Indeed, a more continuous film was formed on the surface with a 24° IL contact angle (Figure 5e) and a continuous film was formed on the surface with a 20° IL contact angle. Similar to the results from IL deposition on SAM-coated

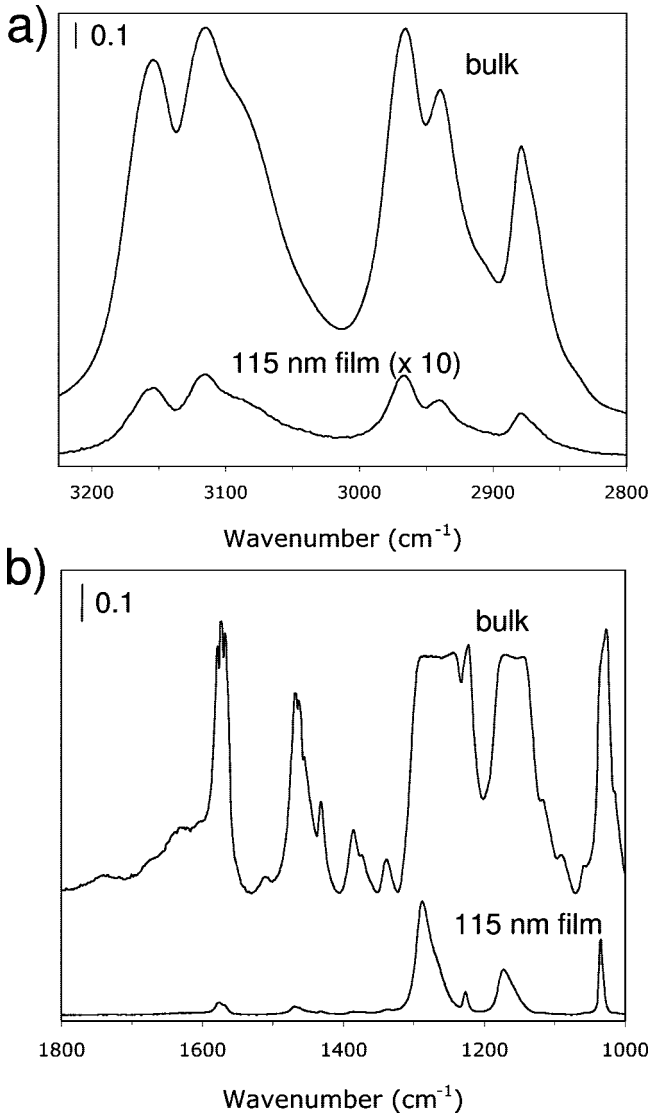

Figure 6. Transmission FTIR spectrum of bulk [bmim][triflate] and a RAIR spectrum of a thin (~115 nm) [bmim][triflate] film cast from solvent are compared. (a) High-frequency region showing peaks that result from C−H stretching in the cation. The spectrum in part a from the thin film is multiplied by 10 for clarity. (b) Mid-frequency region showing peaks in the region of 1600−1300 cm^{-1} that result from C═C and C−N stretching and C−H bending for the bmim cation, and peaks in the region of 1300−1030 cm^{-1} that result primarily from stretching vibrations due to the triflate anion.

gold substrates, surfaces below a critical IL contact angle of ~24(±3)° support a sufficient IL coating by drop casting from ethanol at the reported concentration.

FTIR Analysis of IL Films. A RAIR spectrum of a 115 nm [bmim][triflate] (IL) film on a $HO(CH_2)_{11}S$/Au surface was obtained to provide information on film composition and structure (Figure 6). The IL film was deposited by drop casting from ethanol. For reference, a transmission IR spectrum of the bulk IL was obtained after placing a drop of IL on a NaCl crystal. In the high-frequency region (3300−2800 cm^{-1}) (Figure 6a), the spectrum of the thin (115 nm) film exhibited three major peaks due to hydrocarbon stretching within the butyl side chain of the [bmim] cation, including $\nu_s(CH_3)$ (2882 cm^{-1}), $\nu_{FR}(CH_3)$ (2942 cm^{-1}), and $\nu_a(CH_3)$ (2970 cm^{-1}) that are shifted to higher wavenumber by 1−3 cm^{-1} as compared to the peaks for the bulk film, and two major peaks corresponding to antisymmetric (3118 cm^{-1}) and symmetric (3156 cm^{-1}) stretching from the C−H modes of the imidazolium ring that are at identical positions as those for the bulk film. These vibrations for the cation depend on associations with the anion and are distinct from spectra of other [bmim] salts.[56−58] In the region of 1800−1300 cm^{-1} (Figure 6b), peaks arise from C═C stretching, C−H bending, and C−N ring stretching vibrations in the cation.[58,59]

In the region of 1300−1000 cm^{-1} of Figure 6b, the triflate anion contributes peaks in the spectrum for the thin film due to stretching of $\nu_a(SO_3)$ (1289 cm^{-1}), $\nu_s(CF_3)$ (1229 cm^{-1}), $\nu_a(CF_3)$ (1175 cm^{-1}), and $\nu_s(SO_3)$ (1036 cm^{-1}), which are consistent with previously reported peak assignments for the triflate anion.[60−62] Of particular relevance for the thin film, the sharp $\nu_a(SO_3)$ peak at 1289 cm^{-1} contains a slight shoulder at 1270 cm^{-1} but shows no splitting into two separate components. The transmission spectrum for the bulk film shows a broad $\nu_a(SO_3)$ peak, but the level of splitting is unclear since the peak is over absorbed. To further examine the splitting of a bulk film, we obtained the reflectance spectrum for a ~50 μm [bmim][triflate] film (Supporting Information, Figure S2) prepared onto a $HOC_{11}S$/Au surface from a more concentrated [bmim][triflate]/ethanol solution. This reflectance spectrum for the bulk film does exhibit splitting of the $\nu_a(SO_3)$ mode into peaks at 1255 and 1300 cm^{-1}, with roughly the same broadness as that for the bulk IL film. This splitting of the $\nu_a(SO_3)$ mode arises due to interactions between oxygen of the triflate ion and the counterion. If the strength of this interaction is sufficient, the 2-fold degeneracy of the mode is broken and two separate peaks are observed in the IR spectrum.[60] The absence of the splitting in the $\nu_a(SO_3)$ mode for the spectrum of the thin film suggests a different potential energy environment for the triflate ion in the thin film versus that in the thicker film. This different ionic environment for the thin film may be caused by the larger ratio of SAM/IL and IL/air interfacial area to total film volume for the thin films than for thicker bulk-like films. In effect, the triflate and bmim ions will likely orient with the CF_3 and butyl groups, respectively, at the air/IL interface to minimize unfavorable interactions between the charged moiety and the adjacent phase. This selective orientation may, in turn, affect the approach of ions within the film and the strength of interaction between the ions. Further evidence for a unique environment within the thin film is noted by comparing the large absorbances in Figure 6b for the peaks due to the triflate anion with the much weaker absorbances due to the bmim cation, whereas for the bulk film (Figure 6b) and the ~50 μm film (Figure S2 in the Supporting Information), these absorbances are similar.

Analysis of the droplet structure from molecular simulation of [bmim][triflate] on CH_3- and OH-terminated surfaces provides support for the experimental observations. As shown in Figure 2, in both drops, the butyl chains on the cations point outward, while the imidazolium rings tend to be *shielded* within the surface of the drop. Similarly, a strong orientation effect is evident for anions located in the outer shells of both drops; as shown in Figure 7 the SO_3 groups of the anions are directed toward the center of the drop with the corresponding CF_3 groups pointing outward. However, in the region of contact with the OH-terminated surface the anions appear more randomly distributed (see the IL-monolayer interface shown in Figure 7b). Similar preferred orientation of the cations and anions was observed in simulations of the vapor phase of [bmim][triflate] clusters containing up to 30 ion pairs[54] and is likely due to the charge distribution in these ions, i.e., the positive charge of the bmim cation is concentrated on the methyl-imidazolium group[39] and the negative charge of the triflate anion is concentrated on

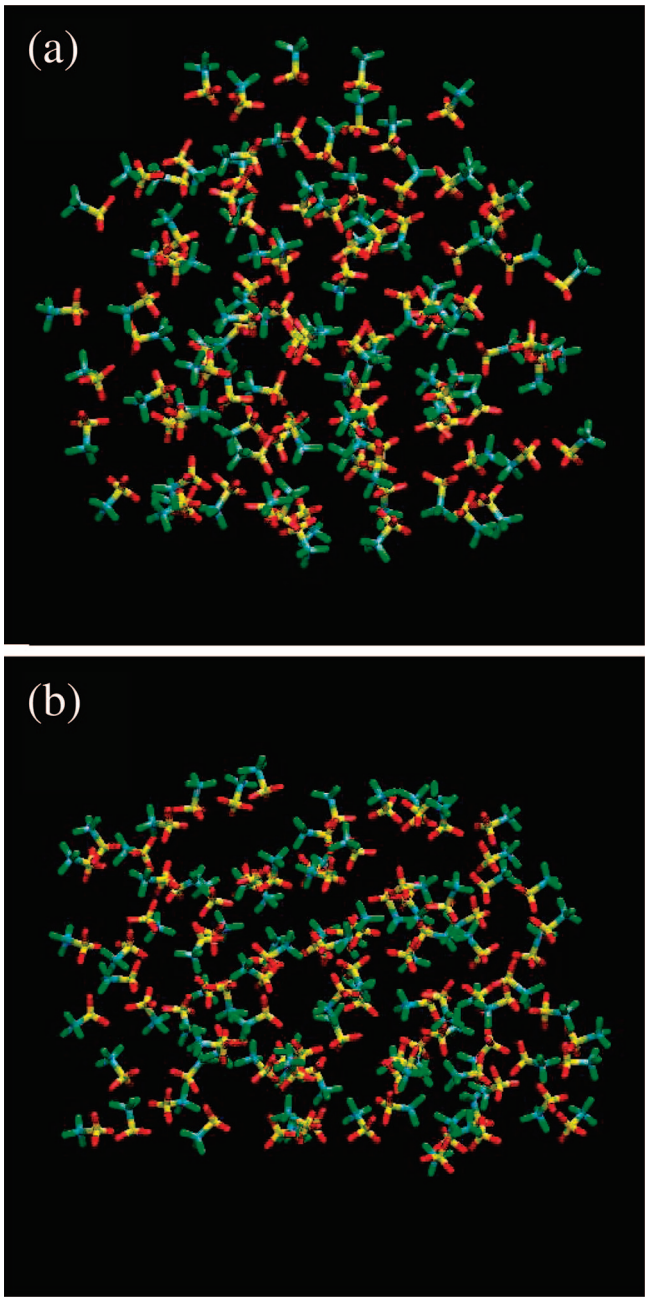

Figure 7. Snapshots showing the orientation of triflate anions within the [bmim][triflate] droplet on (a) CH_3-terminated and (b) OH-terminated monolayer surfaces on silica.

the SO_3 group.[40] In the outer shell, these ions can move and assume the orientation in which their fragments with the higher charge density are directed toward the center of the IL drop. The observed orientation of the triflate anions in the radial direction with the SO_3 groups pointing toward the center of the drop in the outer shells of the IL may induce a different type of structuring within ultrathin IL films.

Conclusions

[bmim][triflate] exhibits contact angles that are stongly influenced by ion pairing within the droplets and are distinct from those exhibited by dicyclohexyl, a dispersive liquid with similar suface tension as the IL. Similar to water, [bmim][triflate] is far less sensitive to compositional changes in hydrophobic surfaces (CH_3 vs CH_2; CF_3 vs CH_3) than is hexadecane or dicyclohexyl. Thin films of [bmim][triflate] were drop cast onto monolayer surfaces of varying energy to investigate the spreading of the IL into thin films. On both Au and Si substrates, the critical surface energy required for the formation of an IL film was characterized by a [bmim][triflate] contact angle of $\leq\sim25(\pm4)°$, which corresponded to an advancing water contact angle of $\leq70(\pm4)°$. Molecular simulations of [bmim][triflate] droplets on hydroxyl- and methyl-terminated monolayers are qualitatively consistent with the experimental observations and show that the higher energy hydroxyl surface induces a perturbation of the characteristic charge alternation of the IL, decreasing the forces of attraction between the ions in the outer shells and reducing the local surface tension in the drop. Comparison of infrared vibrational spectra of the IL in bulk versus as a thin film suggests an interfacially driven structuring of the ions in thinner films ($\sim$100 nm) and is supported by simulations, which show that the CF_3 groups of the triflates orient toward the air interface in droplets.

Acknowledgment. This work was supported by the Office of Naval Research under grant no. N00014-06-1-0624.

Supporting Information Available: The thicknesses of films prepared from *n*-alkyltrichlorosilanes on silicon are plotted as a function of adsorbate chain length and reflectance−absorption infrared spectra are provided for two [bmim][triflate] films, one ultrathin ($\sim$115 nm) and one thick ($\sim$50 μm). This material is available free of charge via the Internet at http://pubs.acs.org.

References and Notes

(1) Weingaertner, H. *Angew. Chem., Int. Ed.* **2008**, *47*, 654–670.
(2) Hoffmann, M.; Heitz, M.; Carr, J.; Tubbs, J. *J. Dispersion Sci. Technol.* **2003**, *24*, 155–171.
(3) Bonhote, P.; Dias, A. P.; Papageorgiou, N.; Kalyanasundaram, K.; Gratzel, M. *Inorg. Chem.* **1996**, *35*, 1168–1178.
(4) Li, J.; Shen, Y.; Zhang, Y.; Liu, Y. *Chem. Commun.* **2005**, 360–362.
(5) Anderson, J. L.; Armstrong, D. W.; Wei, G.-T. *Anal. Chem.* **2006**, *78*, 2892–2902.
(6) Liu, X.; Zhou, F.; Liang, Y.; Liu, W. *Wear* **2006**, *261*, 1174–1179.
(7) Mu, Z.; Zhou, F.; Zhang, S.; Liang, Y.; Weimin, L. *Tribol. Int.* **2005**, *38*, 725–731.
(8) Liu, W.; Ye, C.; Gong, Q.; Wang, H.; Wang, P. *Tribol. Lett.* **2002**, *V13*, 81–85.
(9) Wilkes, J. S.; Zaworotko, M. J. *J. Chem. Soc., Chem. Commun.* **1992**, 965–967.
(10) Liu, W. M.; Ye, C. F.; Gong, Q. Y.; Wang, H. Z.; Wang, P. *Tribol. Lett.* **2002**, *13*, 81–85.
(11) Ye, C. F.; Liu, W. M.; Chen, Y. X.; Yu, L. G. *Chem. Commun.* **2001**, 2244–2245.
(12) Ye, C. F.; Liu, W. M.; Chen, Y. X.; Ou, Z. W. *Wear* **2002**, *253*, 579–584.
(13) Phillips, B. S.; Mantz, R. A.; Trulove, P. C.; Zabinski, J. S. *ACS Symp. Ser.* **2005**, *901*, 244–253.
(14) Yu, G. Q.; Zhou, F.; Liu, W. M.; Liang, Y. M.; Yan, S. Q. *Wear* **2006**, *260*, 1076–1080.
(15) Jimenez, A. E.; Bermudez, M. D.; Iglesias, P.; Carrion, F. J.; Martinez-Nicolas, G. *Wear* **2006**, *260*, 766–782.
(16) Eapen, K.; Patton, S.; Smallwood, S.; Phillips, B.; Zabinski, J. *J. Microelectromech. Syst.* **2005**, *14*, 954–960.
(17) Shaw, D. J. *Colloid and Surface Chemistry*; Butterworth-Heinemann: Oxford, UK, 1992.
(18) Laibinis, P. E.; Palmer, B. J.; Lee, S.-W.; Jennings, G. K. The Synthesis of Organothiols and their Assembly into Monolayers on Gold. In *Thin Films*; Ulman, A., Ed.; Academic Press: Boston, MA, 1998; Vol. 24, pp 1−41.
(19) Gao, L.; McCarthy, T. J. *J. Am. Chem. Soc.* **2007**, *129*, 3804–3805.
(20) Bonhote, P.; Dias, A.; Popageoriou, N.; Kalyanasundaram, K.; Gratzel, M. *Inorg. Chem.* **1996**, *35*, 1168–1178.
(21) Chen, M.-S.; Brandow, S. L.; Schull, T. L.; Chrisey, D. B.; Dressick, W. J. *Adv. Funct. Mater.* **2005**, *15*, 1364–1375.
(22) Stevens, M. *Langmuir* **1999**, *15*, 2773–2778.

(23) Britt, D. W.; Hlady, V. *J. Colloid Interface Sci.* **1996**, *178*, 775–784.
(24) Flinn, D. H.; Guzonas, D. A.; Yoon, R. H. *Colloids Surf., A* **1994**, *87*, 163–176.
(25) McGovern, M. E.; Kallury, K. M. R.; Thompson, M. *Langmuir* **1994**, *10*, 3607–3614.
(26) Fadeev, A. Y.; McCarthy, T. J. *Langmuir* **2000**, *16*, 7268–7274.
(27) Wang, M.; Liechti, K. M.; Wang, Q.; White, J. M. *Langmuir* **2005**, *21*, 1848–1857.
(28) Clear, S. C.; Nealey, P. F. *J. Colloid Interface Sci.* **1999**, *213*, 238–250.
(29) Cassie, A. B. D. *Discuss. Faraday Soc.* **1948**, *3*, 11–16.
(30) P. Villars, L. D. C. *Pearson's Handbook of Crystallographic Data for Intermetallic Phases*, 2nd ed.; ASM International: Materials Park, OH, 1991.
(31) Wyckoff, R. W. G. In *Crystal Structures*; John Wiley & Sons: New York, 1963; Vol. 1, pp 318−319.
(32) Chandross, M.; Grest, G. S.; Stevens, M. J. *Langmuir* **2002**, *18*, 8392–8399.
(33) Stevens, M. J. *Langmuir* **1999**, *15*, 2773–2778.
(34) Maboudian, R. *Surf. Sci. Rep.* **1998**, *30*, 209–270.
(35) Kojio, K.; Ge, S. R.; Takahara, A.; Kajiyama, T. *Langmuir* **1998**, *14*, 971–974.
(36) Tidswell, I. M.; Ocko, B. M.; Pershan, P. S.; Wasserman, S. R.; Whitesides, G. M.; Axe, J. D. *Phys. Rev. B* **1990**, *41*, 1111–1128.
(37) Jorgensen, W. L.; Maxwell, D. S.; Tirado Rives, J. *J. Am. Chem. Soc.* **1996**, *118*, 11225–11236.
(38) Lorenz, C. D.; Webb, E. B.; Stevens, M. J.; Chandross, M.; Grest, G. S. *Tribol. Lett.* **2005**, *19*, 93–99.
(39) Cadena, C.; Maginn, E. J. *J. Phys. Chem. B* **2006**, *110*, 18026–18039.
(40) Lopes, J. N. C.; Padua, A. A. H. *J. Phys. Chem. B* **2004**, *108*, 16893–16898.
(41) Fennell, C. J.; Gezelter, J. D. *J. Chem. Phys.* **2006**, *124*, 234104.
(42) Wolf, D.; Keblinski, P.; Phillpot, S. R.; Eggebrecht, J. *J. Chem. Phys.* **1999**, *110*, 8254–8282.
(43) Tuckerman, M.; Berne, B. J.; Martyna, G. J. *J. Chem. Phys.* **1992**, *97*, 1990–2001.
(44) Berendsen, H. J. C.; Postma, J. P. M.; Vangunsteren, W. F.; Dinola, A.; Haak, J. R. *J. Chem. Phys.* **1984**, *81*, 3684–3690.
(45) Fadeev, A. Y.; McCarthy, T. J. *Langmuir* **2000**, *16*, 7268–7274.
(46) Laibinis, P. E.; Bain, C. D.; Nuzzo, R. G.; Whitesides, G. M. *J. Phys. Chem.* **1995**, *99*, 7663–7676.
(47) Grobe, G. L.; Valint, P. L.; Ammon, D. M. *J. Biomed. Mater. Res. A* **1996**, *32*, 45–54.
(48) Gupta, V. K.; Abbott, N. L. *Phys. Rev. E* **1996**, *54*, R4540−R4543.
(49) Hautman, J.; Klein, M. L. *Phys. Rev. Lett.* **1991**, *67*, 1763–1766.
(50) de Ruijter, M. J.; Blake, T. D.; De Coninck, J. *Langmuir* **1999**, *15*, 7836–7847.
(51) Giovambattista, N.; Debenedetti, P. G.; Rossky, P. J. *J. Phys. Chem. B* **2007**, *111*, 9581–9587.
(52) Srivastava, P.; Chapman, W. G.; Laibinis, P. E. *Langmuir* **2005**, *21*, 12171–12178.
(53) Maginn, E. J. *Acc. Chem. Res.* **2007**, *40*, 1200–1207.
(54) Ballone, P.; Pinilla, C.; Kohanoff, J.; Del Popolo, M. G. *J. Phys. Chem. B* **2007**, *111*, 4938–4950.
(55) quest@surface-tension.de. Surface tension values of common test liquids for surface energy analysis; www.surface-tension.de/, 2006.
(56) Jeon, Y.; Sung, J.; Seo, C.; Lim, H.; Cheong, H.; Kang, M.; Moon, B.; Ouchi, Y.; Kim, D. *J. Phys. Chem. B* **2008**, *112*, 4735–4740.
(57) Jeon, Y.; Sung, J.; Kim, D.; Seo, C.; Cheong, H.; Ouchi, Y.; Ozawa, R.; Hamaguchi, H.-O. *J. Phys. Chem. B* **2008**, *112*, 923–928.
(58) Katsyuba, S. A.; Zvereva, E. E.; Vidis, A.; Dyson, P. J. *J. Phys. Chem. A* **2007**, *111*, 352–370.
(59) Silverstein, R. M.; Webster, F. X.; Kiemle, D. J. *Spectrometric Identification of Organic Compounds*, 7th ed.; John Wiley & Sons, Inc.: New York, 2005.
(60) Huang, W. W.; Frech, R.; Wheeler, R. A. *J. Phys. Chem.* **1994**, *98*, 100–110.
(61) Bernson, A.; Lindgren, J. *Solid State Ionics* **1993**, *60*, 37–41.
(62) Peterson, G.; Jacobson, P.; Torell, L. M. *Electrochem. Acta* **1992**, *37*, 1496–1497.

JP808098W